

Microscopic mechanisms governing exciton-decay kinetics in type-II GaAs/AlAs superlattices

L. P. Fu, F. T. Bacalzo, G. D. Gilliland, R. Chen, and K. K. Bajaj
Department of Physics, Emory University, Atlanta, Georgia 30322

J. Klem
Sandia National Laboratories, Albuquerque, New Mexico 87185

D. J. Wolford
Microelectronics Research Center and Department of Physics, Iowa State University, Ames, Iowa 50011
 (Received 10 February 1995)

We have measured the time- and space-resolved evolution of type-II excitons in GaAs/AlAs superlattices with various AlAs layer thicknesses, at temperatures ranging from 1.8 to 30 K. Our photoluminescence (PL) time decay and transport results demonstrate that the exciton-decay kinetics at low temperatures are entirely determined by intrinsic radiative recombination, whereas at higher temperatures, the PL time decays are dominated by nonradiative defect trapping processes. We show that these nonradiative decays do not occur within the layers but are instead localized at the heterointerfaces. The measured lifetimes at 30 K are consistent with our model calculations based on this interpretation. Furthermore, the superlattice and interface-disorder-induced Γ - X mixing potentials are determined from our low-temperature exciton lifetimes to be 1.3 and 0.2 meV, respectively.

I. INTRODUCTION

Although the electronic energy states of type-II $(\text{GaAs})_m/(\text{AlAs})_n$ superlattices ($m < 13$ and $n > 6$) are fairly well understood, there is still considerable confusion about the recombination processes of excitons in these structures. In type-II $(\text{GaAs})_m/(\text{AlAs})_n$ superlattices excitons are formed by the Coulomb interaction of holes residing at the Γ point of the GaAs layers with electrons located at the X conduction-band edges of the AlAs layers.^{1,2} These type-II excitons are thus indirect in both real and momentum space. The finite oscillator strength of the no-phonon line commonly observed in the photoluminescence (PL) spectrum is generally attributed to the k -space momentum mixing of the Γ and X conduction-band states (Γ - X mixing) by various mechanisms, such as the superlattice potential and/or interface disorder or potential fluctuations at the heterointerfaces.³⁻⁸ Furthermore, the conduction-band X valleys of the AlAs layers split into $X_{X,Y}$ and X_Z electronic states due to quantum confinement and strain. It has been demonstrated that in samples with AlAs-layer thicknesses $> 55 \text{ \AA}$, the $X_{X,Y}$ states are lower in energy than the X_Z states, but when the AlAs thicknesses are $< 55 \text{ \AA}$, X_Z becomes the electronic ground state.^{9,10} Since the recombination of these doubly forbidden excitons relies strongly on the amount of Γ - X mixing, the radiative lifetime of these type-II excitons should show a strong dependence of both the AlAs thickness and the disorder at the heterointerfaces. The decay kinetics of these type-II excitons should also be very sensitive to the microscopic structure at the interfaces because of the large spatial overlap of these excitons with the heteroin-

terfaces. However, systematic studies of the microscopic mechanisms governing the exciton kinetics are still lacking in the literature.

In these type-II superlattices it is universally observed that the PL lifetime decreases rapidly with increasing temperature¹¹ and, concomitantly, the PL intensity becomes thermally quenched. Different theories were thus proposed¹²⁻¹⁵ to explain the exciton-decay kinetics, and it is generally accepted that the decrease in lifetime results from thermal detrapping of localized excitons. For instance, Angell and Sturge¹⁵ recently proposed a theory of exciton decay in type-II structures based upon an exciton hopping process, with resulting excitonic optical transitions being motionally averaged over a distribution of decay rates as temperature is increased and thermal delocalization sets in. However, this model omits the effects of nonradiative decay and does not quantify the extent of spatial transport, and therefore does not explain the quenching of the PL with increasing temperature. On the other hand, Gilliland *et al.*¹⁶ have already directly measured such exciton spatial motion in type-II structures, thereby proving the validity of a thermal detrapping view of the localized excitons and further demonstrating the importance of the nonradiative decay due to trapping of mobile excitons by defects.

In this paper, we present a systematic study of the exciton-decay kinetics and transport in type-II GaAs/AlAs superlattices with AlAs-layer thicknesses varying from 20 to 80 \AA . We find that the low-temperature ($T < 10 \text{ K}$) decay kinetics are governed by *radiative recombination*, whereas the higher-temperature ($T \sim 30 \text{ K}$) decays are dominated by the *nonradiative trapping process* discussed in Ref. 16. These unequivocal

conclusions are only possible through measurements of *both* exciton-decay kinetics and transport. Model calculations were performed and after comparison of the low-temperature lifetimes, individual strengths of the Γ - X mixing due to both the superlattice potential and the heterointerfacial roughness (interface-disorder) were determined. We thus find in these samples that such superlattice mixing potential is significantly larger than the interface-disorder-induced potential. To the best of our knowledge, this is the first direct measurement of the interface-disordered Γ - X mixing potential and the first quantitative comparison of the importance of the two mixing mechanisms. In addition, through detailed comparison of our theoretical model to the measured lifetimes and diffusivities from different samples at $T=30$ K, we have demonstrated that the nonradiative decay process limiting the higher-temperature lifetimes in these structures is closely related to the spatial overlap of the excitons with the defects localized near the heterointerfaces.

II. EXPERIMENT

In an effort to understand the microscopic mechanisms governing the exciton-decay kinetics, we have performed PL, PL time-decay, and time-resolved PL imaging experiments. Exciton recombination was measured using time-correlated single-photon counting, while exciton transport was measured using an all-optical, time-resolved PL-imaging technique, where PL is both temporally and spatially resolved, and which relies on confocal laser excitation and imaging of the mobile, photoexcited excitons.¹⁷ Photoluminescence was excited by a cw Ar⁺-laser-pumped mode-locked Ti³⁺: sapphire laser, which was frequency doubled, and pulse picked to lower the repetition rate appropriate to the PL decay lifetime. Near diffraction limit laser spot sizes (~ 3 μm) were achieved with a temporal and spectral resolution of ~ 500 ps and ~ 0.1 \AA , respectively.

The samples were undoped GaAs/AlAs superlattices grown at 600°C by molecular-beam epitaxy (MBE). GaAs layers in all samples are nominally 30 \AA thick in all samples, while AlAs layers were intended to vary from 20 to 80 \AA (each sample was also grown on top of a 1- μm -thick GaAs buffer layer). Specific samples, on which we present data here, contain—by MBE-growth-rate calibrations—GaAs (AlAs) layer thicknesses of 35 \AA (20 \AA), 30 \AA (50 \AA), and 25 \AA (80 \AA), and are labeled G0002, BL141, and G0169, respectively; hence, the actual GaAs-layer thicknesses were indeed maintained nearly fixed across this series.

III. RESULTS AND DISCUSSIONS

It has been established that the relative intensity of the no-phonon line (and its corresponding phonon replicas) reflects not only the extent of Γ - X mixing occurring within the type-II superlattice, but also the symmetry of the X conduction-band edge electronic ground state.^{9,10} Figure 1 displays the cw PL spectra of each sample at 10 K. Those with narrow AlAs-layer thicknesses (20 and 50 \AA), in which X_Z is the electronic ground state, exhibit

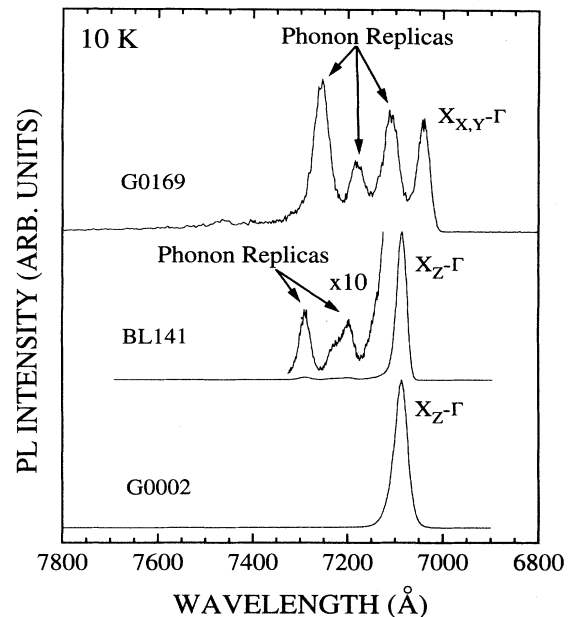


FIG. 1. Photoluminescence spectra from samples G0169, BL141, and G0002 at 10 K. Spectra are offset vertically and normalized for clarity.

strong no-phonon X_Z - Γ transitions and weaker phonon replicas. In contrast, samples with thicker AlAs-layer thicknesses (> 65 \AA), in which $X_{X,Y}$ is the electronic ground state, exhibit a weaker no-phonon $X_{X,Y}$ - Γ emission line and more intense phonon replicas (relative to the no-phonon line). Such observations qualitatively suggest that a larger Γ - X mixing potential exists in samples with narrower AlAs-layer thicknesses. Detailed mechanisms responsible for any quantitatively differing amounts of Γ - X mixing in these samples will be addressed later in connection with the low-temperature PL time decays. Further, concerning the no-phonon PL lines, we find that with increasing temperature the linewidths increase slightly, while peak emission energies remain largely invariant. Moreover, under pulsed excitation, the overall PL intensities decrease drastically with increasing temperature—a result implying the existence of a strong temperature-dependent nonradiative^{11–13,16} decay process.

Photoluminescence time decays of the no-phonon emission versus temperature were measured versus temperature. Here, for all samples, we find at low temperatures the decays are long and nonexponential, and with increasing temperature they become faster and rigorously exponential. This universally observed behavior is illustrated in Fig. 2 for sample G0169. The time-decay data were empirically fit (shown as solid lines) using the sum of an exponential function and a bimolecular expression, and the corresponding lifetimes were thus derived from the long-time tail of the decays.

Figure 3 shows such lifetimes deduced from least-squared fits to the long-time exponential tails of these de-

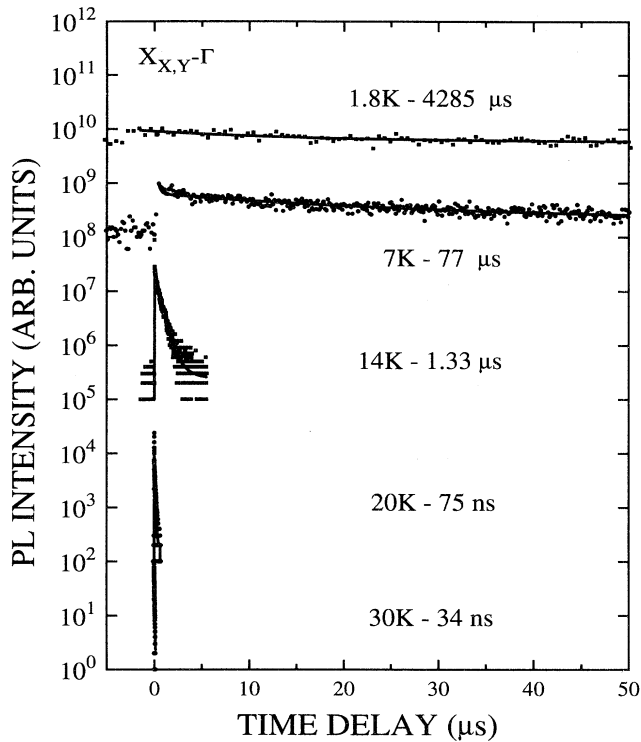


FIG. 2. Temperature dependence of decay kinetics for sample G0169. The solid lines are least-square fits to the data. Data are offset vertically for clarity.

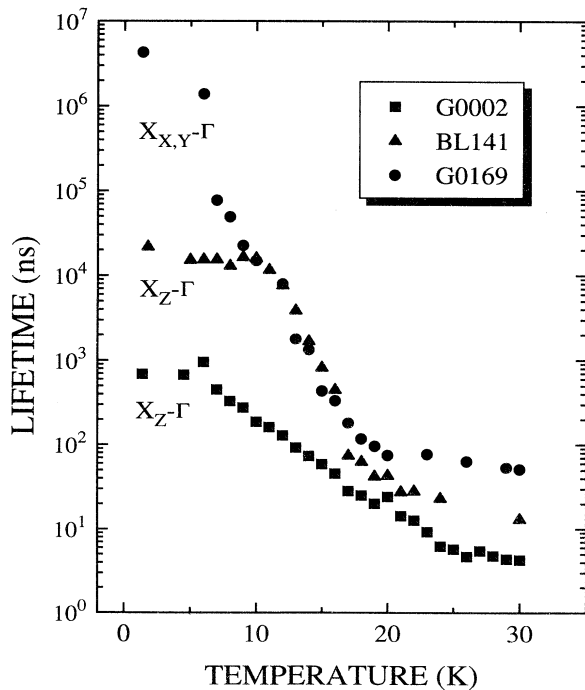


FIG. 3. Lifetime vs temperature for samples with various AlAs-layer thicknesses.

cays. As is made clear in Fig. 2, these derived lifetimes exhibit, in all samples, a rapid decrease in magnitude as temperature is increased. Indeed, for example, sample G0169 exhibits a truly remarkable *5-order-of-magnitude decrease in lifetime between 1.8 and 30 K*. Further, at all temperatures, the derived lifetimes systematically increase in magnitude for increasing AlAs-layer thicknesses. However, the *quantitative differences* in lifetimes among the three samples *decrease* as temperature increases, a result possibly indicative of the dominance of a decay mechanism at higher temperatures, which is relatively less sensitive to the sample structure.

In an effort to further understand the origin of the decay kinetics, we have used our combination time- and space-resolved PL imaging technique, to measure the *lateral transport* of these type-II excitons *along the heterointerfaces*. Figure 4 depicts the thus-derived monotonic increase in excitonic diffusivities with temperature for our three representative samples. The measured diffusivities range from 10^{-3} cm²/s at 1.8 K to 100 cm²/s at 50 K. These results clearly indicate the photoexcited type-II excitons are, at lowest temperatures, spatially localized and at higher temperatures become thermally activated to mobile states. Once mobile, these interface-straddling excitons may then diffuse and possibly encounter defects and recombine nonradiatively. Our theoretical estimates based on the thermal detrapping model¹⁶ described above show the sheet density of such deleterious nonradiative defects to be nonetheless ostensibly relatively low, $\sim 10^6$ – 10^7 cm⁻².

Thus, we may conclude that, at least at low temperatures, in our type-II superlattice systems excitons are spatially localized and are therefore apparently relatively in-

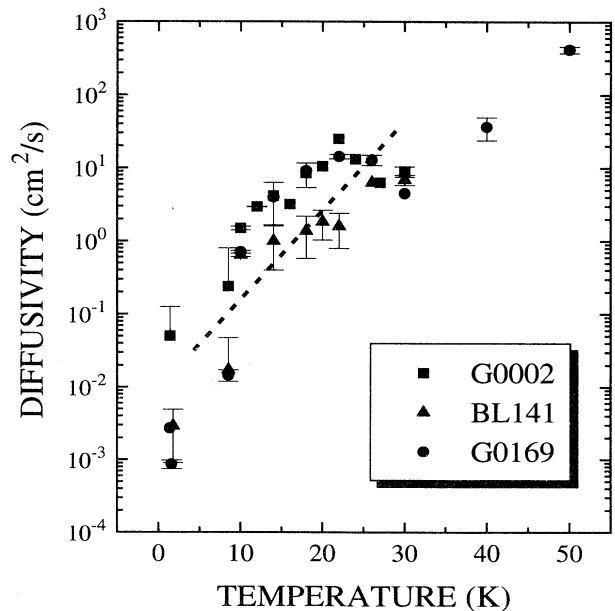


FIG. 4. Measured diffusivity vs temperature for samples G0169, BL141, and G0002. The dashed line is just a guide to the eye.

sensitive to nonradiative decay at such sparsely arrayed defect sites. It should be noted that this qualitative but significant conclusion is made possible only because of our unique ability to quantify the excitonic transport and nonradiative defect density (e.g., the average sheet-defect spacing is $\sim 3 \mu\text{m}$, as compared to the approximate excitonic radius of 100 \AA). Thus, the observed decay kinetics at lowest temperatures are primarily determined by the *intrinsic* cross-interface and cross- k -space radiative recombination of the type-II excitons. The nonexponential decays found at these lowest temperatures are consistent with there being heterointerfacial disorder-induced inhomogeneous broadening of the PL linewidth and a concomitant *distribution* of radiative rates, despite the fact that these superlattices are made up of binary compounds. It should also be noted in this context that the lifetimes derived for long-time behavior at $T=1.8 \text{ K}$ are 4285 , 21.5 , and $0.687 \mu\text{s}$ for samples G0169, BL141, and G0002, respectively. This relatively large variation (4 orders of magnitude) at lowest temperatures most probably reflects the combined differences in electronic states (conduction-band ground state of X_Z versus $X_{X,Y}$),^{9,10} the microstructural dependence of the wave-function overlap between electrons and holes upon superlattice composition, and the variances in the magnitude of the Γ - X mixing potential, which hybridizes the AlAs X -electron states. The PL time-decay data suggest that the type-II excitonic lifetimes decrease rapidly with decreasing AlAs-layer thickness, as a result of the increased amount of Γ - X mixing.

In order to identify the underlying mechanisms and magnitudes of the mixing potentials, we have performed calculations based on first-order perturbation theory of the exciton envelope functions. For this purpose, the electron portion of the excitonic wave function is taken, to a first approximation, as a linear combination of the Γ ($k=0$) and X wave functions:

$$\Psi_e = c_\Gamma \Psi_c^\Gamma + c_x \Psi_c^X, \quad (1)$$

where $c_x = c_\Gamma \langle \Psi_c^X | V | \Psi_c^\Gamma \rangle / (E_\Gamma - E_X)$, and c_Γ may be determined by appropriate normalization of the electron wave function, and for which only k -space mixing with the lowest confined Γ ($k=0$) state is taken into account. The matrix element, $A = \langle \Psi_c^X | V | \Psi_c^\Gamma \rangle$, then represents the *total* Γ - X mixing via a variety of mechanisms—including, most importantly, interface-disorder scattering (note that to this order in perturbation theory, we do not distinguish among the anisotropic interface-disorder scattering mechanisms) and the superlattice-modulation potential (i.e., “zone-folding” effect). The radiative recombination rate of the type-II excitons, including the overlap of the electronic envelope functions in the AlAs and GaAs layers, can then be described by the matrix element,

$$M_{\text{II}} \approx M_{\text{I}} \langle \Psi_{\text{AlAs}}^{\text{env}} | \Psi_{\text{GaAs}}^{\text{env}} \rangle (A / \Delta E), \quad (2)$$

where $\Delta E = E_\Gamma - E_X$ is the energy separation between the Γ and X states, M_{I} is the optical-transition matrix element for a type-I Γ -electron ($k=0$) to Γ -hole transition, and $\Psi_{\text{GaAs}}^{\text{env}}$ and $\Psi_{\text{AlAs}}^{\text{env}}$ are the slowly varying electron

envelope functions in the GaAs and AlAs layers, respectively. The radiative lifetime is inversely proportional to the square of the matrix element, and is given by

$$\tau_{\text{II}} \approx \tau_{\text{I}} \left[\frac{\Delta E}{(A \langle \Psi_{\text{AlAs}}^{\text{env}} | \Psi_{\text{GaAs}}^{\text{env}} \rangle)} \right]^2. \quad (3)$$

The energy separation (ΔE) between the Γ and X states was determined from our PL measurements, and the overlap integral of the electron envelope function was calculated using a Kronig-Penney model. Based on data for the recombination lifetime in typical type-I quantum wells,¹⁸ we may here assume the type-I superlattice lifetime (τ_{I}) of 250 ps. Using Eq. (3) and the measured lifetimes at $T=1.8 \text{ K}$, we have determined the total derived Γ - X mixing potentials for the G0002, BL141, and G0169 samples to be 1.5, 1.5, and 0.2 meV, respectively. Thus, the deduced mixing potential for sample G0169 ($25 \text{ \AA}/80 \text{ \AA}$) is much smaller than that of the other two samples.

This marked difference can be reasonably explained as resulting from the $X_{X,Y}$ symmetry of the lowest electronic state of sample G0169, in which the superlattice Γ - X mixing is *not effective* (due to symmetry) since the periodic potential is primarily along the z direction and thus the primary mixing mechanism is due to the disorder scattering associated with potential fluctuations localized near the heterointerfaces (e.g., binary-binary intermixing forming an intermediate “alloy” region, interface roughness induced by step-height fluctuations, etc.). In contrast, in the two companion samples (G0002 and BL141) in which X_Z is the electronic ground state, the Γ - X mixing mechanism involves *both* the superlattice-modulation potential and the interface disorder. Although the low-temperature lifetimes for samples G0002 and BL141 are quite different (a factor of 30), we nonetheless obtained an identical mixing potential (1.5 meV) for them, as a result of properly accounting for the structural dependence of the wave functions. This further supports our assertion that the low-temperature decay kinetics can be realistically described entirely by the radiative recombination of the localized type-II excitons.

Assuming the interface disorder does indeed induce Γ - X mixing, and that its magnitude is the same in all samples studied here (i.e., the interfacial disorder or roughness is qualitatively similar throughout—as supported by the similar PL linewidths), we calculate the superlattice Γ - X mixing potential (SMP) and interface-disorder Γ - X mixing potential (IDMP) to be 1.3 and 0.2 meV, respectively. To place these values in context, several other reports of the SMP values might be helpful to note. For example, among these are Γ - X SMP derivatives Meynadier *et al.*³ used in their description of the indirect-to-direct crossing induced by an electric field and leading to SMP values of 1–3 meV for structures with periods ranging from 38 to 88 \AA . Another is that quoted by Maaref *et al.*⁴ who derived a value of 4 meV for 26- and 62- \AA AlAs-layer thicknesses. Still further, Dawson *et al.*¹³ obtained a value of some 3 meV for structures with AlAs-layer thicknesses ranging from 19 to 41 \AA . And finally, van Kesteren *et al.*⁹ reported a $<0.2 \text{ meV}$

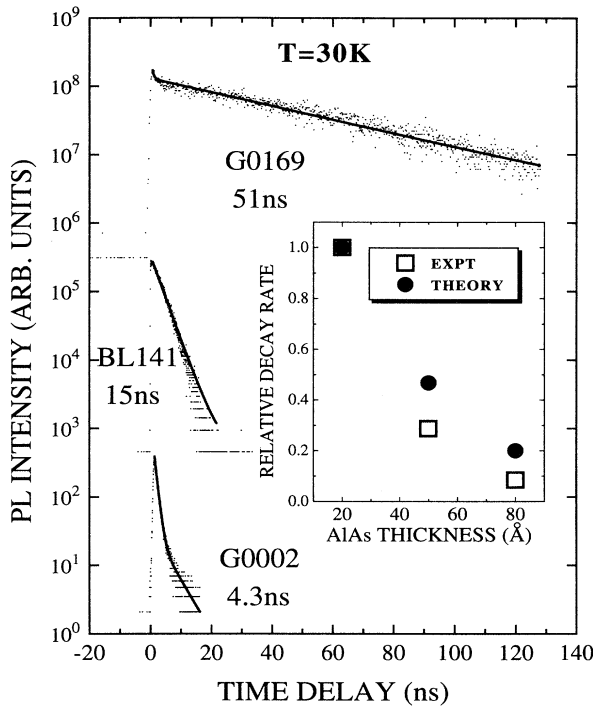


FIG. 5. Photoluminescence time decays for samples G0169, BL141, and G0002 at 30 K. The solid lines are exponential fits to the data. The relative decay rates (open square, experiment; solid circle; theory) vs AlAs thickness are shown in the inset.

mixing potential between the X_X and X_Y states for structures with AlAs thicknesses > 100 Å. In contrast there are no reports, as far as we are aware, of interface-disorder mixing potentials for coupling $X_{X,Y}$ to Γ . However, Tribe, Klipstein, and Smith¹⁹ deduced a value of < 0.75 meV for the X_Z to $X_{X,Y}$ IDMP, a value that is close to ours despite a physically different coupling mechanism from that reported here. In these contexts the relatively small value we derived for the IDMP is possibly a reflection of the high interfacial quality of our MBE superlattices. To the best of our knowledge, this is the first measurement of this interface-disorder Γ - X mixing potential. Since such mixing potentials will most certainly vary from sample to sample with differing growth conditions—we might conclude that its magnitude may, in fact, be used as a quantitative criterion for evaluating and comparing heterointerfacial quality. Further investigation of the relation between low-temperature lifetimes and various sample growth conditions, such as growth interrupts, are being pursued and will be reported in a later publication.²⁰

In comparison to the low-temperature 1.8 K decay kinetics, at higher temperatures (e.g., $T \sim 30$ K) our measured decays become almost entirely exponential, and significantly shorter—as shown in the 30-K time-decay comparisons in Fig. 5. This may be accounted for by recognizing that excitons which readily become localized at lowest temperatures, at increasing temperatures thermally populate the mobile states. These mobile exci-

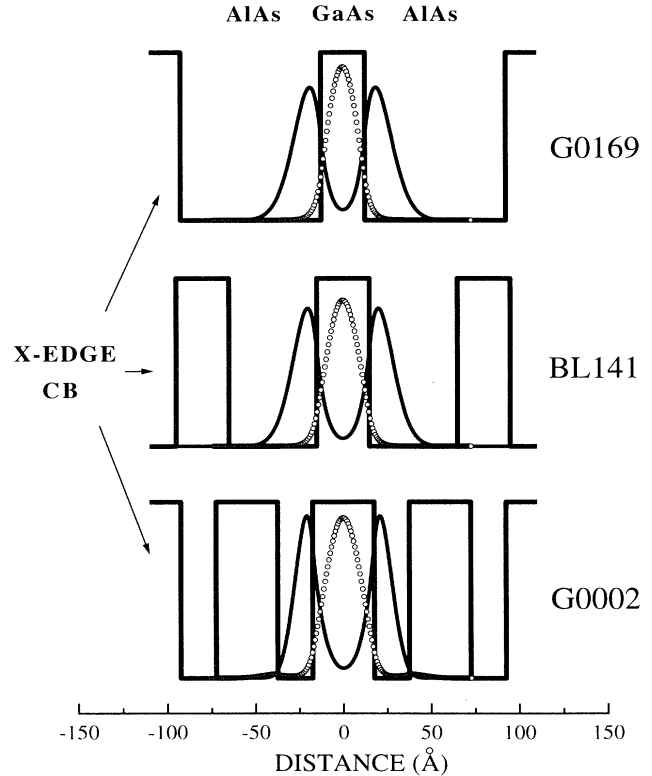


FIG. 6. Calculated probability densities for the electron (solid lines) and hole (open circles) components of the type-II excitons in samples G0169, BL141, and G0002.

tions may then spatially diffuse until they encounter non-radiative defects that would efficiently recapture the excitons, thus leading to a quenching of the PL intensity and a corresponding drastic shortening of its time decay. Hence, we may then conclude the lifetimes derived at higher temperatures are only apparent (rather than intrinsic), instead being governed (if not wholly determined) by nonradiative decay which is enhanced by the increased diffusivity of these excitons. The data in Fig. 4 representing the temperature dependence of such exciton diffusion are consistent with this interpretation. In contrast, at lowest temperature (e.g., $T = 1.8$ K), where excitonic diffusivity was found to be negligible, this nonradiative decay is of little or no consequence.

A further remark concerning the decays of Fig. 5 is the relatively small, but genuine, systematic decrease in lifetime with decreasing AlAs-barrier thickness. To possibly understand this apparent structural dependence of the observed nonradiative decay, one may look to the possible microscopic origin of the dominating nonradiative trapping centers. Since these type-II excitons indeed “straddle” the heterointerfaces, exciton recombination should be extremely sensitive to interfacial defects and their microstructure. This is evident by the larger excitonic PL linewidths of type-II structures compared to type-I structures prepared under otherwise identical growth conditions.

In an effort to elucidate the microscopic mechanism

governing the decay kinetics at higher temperatures, we have performed variational calculations²¹ within the framework of the effective-mass approximation and obtained the type-II excitonic wave functions for these structures. Figure 6 shows the computed electron (solid lines) and hole (open circles) probability densities that comprise the type-II excitons in these three samples. It clearly demonstrates the microstructural dependence of the overlap of the exciton wave function upon the details of the heterointerfaces. As may be easily noted, the hole wave functions are centered and mostly confined within the GaAs layers, and are approximately the same for the three structures. In contrast, however, the electron wave functions peak at positions very close to the heterointerfaces, and hence, the probability of finding electrons at the interfaces might be expected to, and does in the calculation, show a strong dependence on the AlAs-layer thickness. We have also computed the *fractional probability* of these excitons existing (combined electron-hole probabilities) *within a monolayer* of the heterointerfaces. These resulting fractional values are found to be 0.045, 0.027, and 0.018 for samples G0002, BL141, and G0169, respectively. Multiplying these values against their corresponding measured diffusivities of 8.9, 6.9, and 4.5 cm²/s, respectively, we have computed the relative non-radiative decay rates (with respect to that of sample G0002), assuming the same heterointerfacial sheet-defect density ($\sim 10^7$ cm⁻²) for all three samples. These values are shown in the inset of Fig. 5 together with their corresponding experimental values, and show reasonable agreement with the data. From these results, we may conclude that the excitonic nonradiative decay rate de-

pends most strongly on the overlap of the exciton wave function with the heterointerfaces.

IV. CONCLUSIONS

In conclusion, we have shown that the low-temperature (<5 K) decay kinetics of type-II GaAs/AlAs superlattices may be considered to be totally governed by *radiative recombination*. Further, the Γ -X mixing responsible for the prominently observed non-phonon emission is determined by the superlattice modulation potential in samples with X_Z being the electronic ground state. The deduced superlattice mixing potential, which is obtained from samples with X_Z being the electronic ground state, is in accordance with that reported in literature. From the sample in which the electronic ground state is, in contrast, $X_{X,Y}$, we have determined the Γ -X interface-disorder mixing potential to be 0.2 meV. Further, we have also demonstrated that the high-temperature (e.g., 30 K) decay kinetics are almost entirely governed by extrinsic defect-induced *nonradiative recombination* that occurs within the heterointerfacial plane. A concomitant observed systematic trend in PL lifetimes at 30 K for different samples is also consistent with theoretically modeled cross-interface and cross- k -space excitonic wave functions.

ACKNOWLEDGMENTS

The authors are very grateful to J. Carr, B. Puckett, and H. Dale for their technical assistance. This work was supported in part by Air Force Office of Scientific Research under Grant No. AFOSR-91-0056, and the U.S. DOE under Contract No. DE-AC04-94AL85000.

¹E. Finkman, M. D. Sturge, M. H. Meynadier, R. E. Nahory, M. C. Tamargo, D. M. Hwang, and C. C. Chang, *J. Lumin.* **39**, 57 (1987).

²B. A. Wilson, *IEEE J. Quantum Electron.* **QE-14**, 1763 (1988).

³M. H. Meynadier, R. E. Nahory, J. M. Warlock, M. C. Tamargo, J. L. de Miguel, and M. D. Sturge, *Phys. Rev. Lett.* **60**, 1338 (1988).

⁴M. Maaref, F. F. Charfi, D. Scalbert, C. Benoit à la Guillaume, and R. Planel, *Solid State Commun.* **81**, 35 (1992).

⁵D. Z.-Y. Ting and Y. C. Chang, *Phys. Rev. B* **36**, 4359 (1987).

⁶Y. Lu and L. J. Sham, *Phys. Rev. B* **40**, 5567 (1989).

⁷I. Morrison, L. D. L. Brown, and M. Jaros, *Phys. Rev. B* **42**, 11 818 (1990).

⁸W. Ge, W. D. Schmidt, M. D. Sturge, L. W. Pfeiffer, and K. W. West, *J. Lumin.* **48**, 759 (1991).

⁹H. W. van Kesteren, E. C. Cosman, P. Dawson, K. J. Moore, and C. T. Foxon, *Phys. Rev. B* **39**, 13 426 (1989).

¹⁰W. Ge, M. D. Sturge, W. D. Schmidt, L. N. Pfeiffer, and K. W. West, *Appl. Phys. Lett.* **57**, 55 (1990).

¹¹F. Minami, K. Hirata, K. Era, T. Yao, and Y. Masumoto, *Phys. Rev. B* **36**, 2875 (1987).

¹²J. Ihm, *Appl. Phys. Lett.* **50**, 1068 (1987).

¹³P. Dawson, K. J. Moore, C. T. Foxon, G. W. 't Hooft, and R. P. M. van Hal, *J. Appl. Phys.* **65**, 3606 (1989).

¹⁴M. D. Sturge, J. L. Mackay, C. Maloney, and J. K. Pribram, *J. Appl. Phys.* **66**, 5639 (1989).

¹⁵J. F. Angell and M. D. Sturge, *Phys. Rev. B* **48**, 4650 (1993).

¹⁶G. D. Gilliland, A. Antonelli, D. J. Wolford, K. K. Bajaj, J. Klem, and J. A. Bradley, *Phys. Rev. Lett.* **71**, 3717 (1993).

¹⁷G. D. Gilliland, D. J. Wolford, T. F. Kuech, and J. A. Bradley, *Appl. Phys. Lett.* **59**, 216 (1991).

¹⁸J. Feldman, G. Peter, E. O. Göbel, P. Dawson, K. J. Moore, C. T. Foxon, and R. J. Elliott, *Phys. Rev. Lett.* **59**, 2337 (1987).

¹⁹W. R. Tribe, P. C. Klipstein, and G. W. Smith, in *Proceedings of the 22nd International Conference on the Physics of Semiconductors, Vancouver, Canada, 1994*, edited by D. J. Lockwood (World Scientific, Singapore, 1995), pp. 759–762.

²⁰T. Chang, L. P. Fu, F. T. Bacalzo, G. D. Gilliland, D. J. Wolford, K. K. Bajaj, A. Antonelli, R. Chen, J. Klem, and M. Hafich, *J. Vac. Sci. Technol.* (to be published).

²¹S. V. Branis, J. Cen, and K. K. Bajaj, *Phys. Rev. B* **44**, 11 196 (1991).